

## Positronium formation in positron-metastable-helium collisions

J. Hanssen and P. A. Hervieux

*Laboratoire de Physique Moléculaire et des Collisions, Institut de Physique Rue Arago, Technopôle 2000, 57078 Metz Cedex 3, France*

O. A. Fojón and R. D. Rivarola

*Instituto de Física Rosario, CONICET-UNR and Escuela de Ciencias Exactas y Naturales, Facultad de Ciencias Exactas, Ingeniería y Agrimensura, Avenida Pellegrini 250, 2000 Rosario, Argentina*

(Received 25 July 2000; published 6 December 2000)

Positronium formation in the transfer-excitation reaction of positrons impacting on singlet and triplet metastable He( $1s2s$ ) is studied at intermediate and high impact energies within the framework of a four-body version of the continuum distorted wave-final state model. Cross sections for selective final states of the residual target as well as total cross sections and polarization fraction of the  $2p-1s$  multiplet line of He<sup>+</sup> are computed by using a partial-wave technique. For  $2p$  final states of He<sup>+</sup> cross sections exhibit interference patterns.

DOI: 10.1103/PhysRevA.63.012705

PACS number(s): 34.70.+e, 36.10.Dr, 36.40.Sx, 36.40.Wa

### I. INTRODUCTION

In the last years, collisions of positrons impacting on atoms (ions) have been the subject of intense theoretical and experimental research [1,2]. The availability of more intense and stable positron beams has partially promoted these works. The formation of positronium atoms (bound system consisting of a positron and an electron) through electron capture is one of the possible final channels of the positron-atom reaction. This reaction is of interest in many fields such as astrophysics, atomic physics, and material science.

In particular, a three-body continuum distorted wave-final state (CDW-FS) model was developed to study charge exchange with positronium formation in collisions of fast positrons with hydrogenic [3–5] targets. A similar approximation was previously developed to treat the case of hydrogen targets [6]. Later, the CDW-FS approximation was employed to study alkaline-earth-metal targets [7] and compared with success to available experimental data. A four-body Coulomb-Born approximation (CBA) was also introduced [8] to analyze the positronium formation by impact of positrons on helium atoms in their ground state showing also a good agreement with the experiment. In addition to the experimental work [9,10], several theoretical models were developed to treat this collision system. Among them, classical trajectory Monte Carlo techniques [11], distorted-wave approximations [12], and close coupling approximations (CCA) [13–17]. In a recent work (hereafter I) [18], a four-body CDW-FS-4b model has been developed to study positronium formation in the transfer-excitation process with helium and alkaline-earth metals in their ground state.

Here, the CDW-FS-4b model is applied to the case of helium targets in the  $2^1S(1s2s)$  (singlet) and  $2^3S(1s2s)$  (triplet) excited states. Ionic metastable states are common in all quasi-two-electron systems. In the case of He-like ions, the  $2^3S$  term presents a long lifetime ( $\tau \geq 10^{-4}$  s for species with nuclear charge  $Z_T < 10$ ) decaying into the ground state  $1^1S(1s^2)$  through magnetic dipole transitions [19]. These excited states may be obtained in a considerable amount through excitation by electron impact [20]. They may also be

prepared by using crossed beam devices although in this way the relative proportions of metastable states are quite lower. Finally, beams of metastable states of weak intensity may be produced through electron capture by impact of slow He<sup>+</sup> over alkaline targets. By choosing conveniently the alkaline-earth-metal atoms, the beams may be prepared even in a definite spin state.

CDW-FS-4b and CBA differential and total-cross-sections for positronium formation in the ground state are calculated for metastable singlet and triplet states of helium targets by using a partial-wave technique previously developed in Ref. [4]. The CDW-FS-4b approximation is expected to be valid for at high impact energies, i.e., for impact velocities larger than the mean initial orbital velocity of the target electrons. Atomic units will be used except as otherwise stated.

### II. THEORETICAL METHOD

Let us consider the electron-capture process with positronium-formation in positron-metastable helium collisions at intermediate and high impact energies. The CDW-FS-4b approximation introduced in I is used to study this reaction. The initial wave function is chosen as [4]

$$\xi_{\alpha}^{(+)} = {}^S\Phi_{\alpha}(\mathbf{r}_1, \mathbf{r}_2) \mathcal{F}_{\mathbf{k}_{\alpha}}^{(+)}(\mathbf{R}) \quad (1)$$

Coordinates are sketched in Fig. 1.  $M_T$  indicates the nuclear target mass ( $M_T \gg 1$ ).

${}^S\Phi_{\alpha}$  is the initial bound wave function of metastable helium corresponding to the triplet ( $S=1$ ) or singlet ( $S=0$ ) state and is given by

$$\begin{aligned} {}^S\Phi_{\alpha}(\mathbf{r}_1, \mathbf{r}_2) = & \frac{1}{\sqrt{2}} \{ {}^S\varphi_{1s}(\mathbf{r}_1) {}^S\varphi_{2s}(\mathbf{r}_2) \\ & + (-1)^{SS} \varphi_{1s}(\mathbf{r}_2) {}^S\varphi_{2s}(\mathbf{r}_1) \} \quad (2) \end{aligned}$$

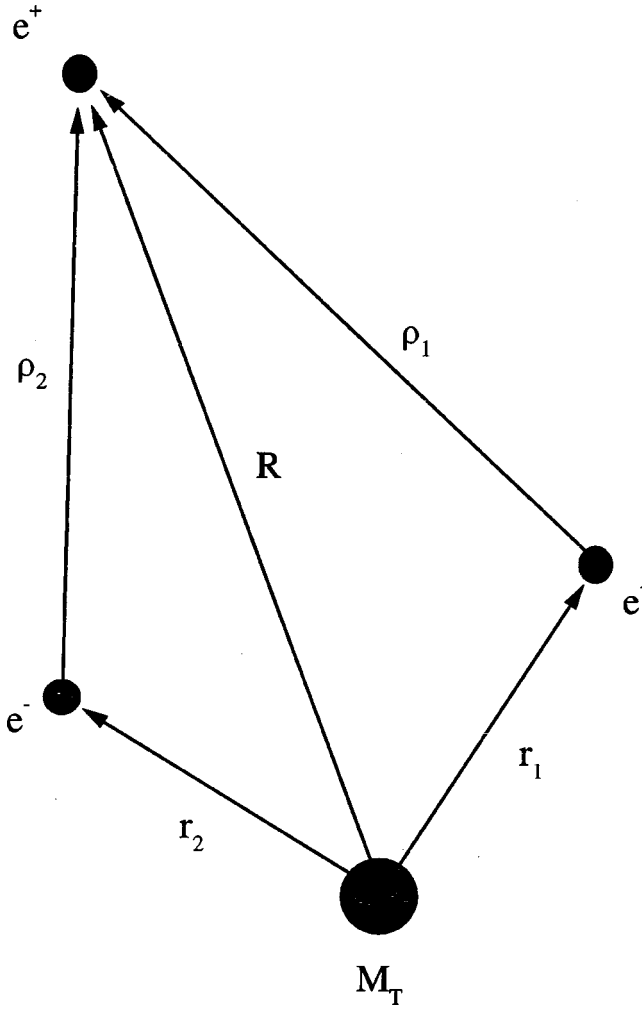


FIG. 1. Coordinates used in the text.

${}^S\varphi_i$  ( $i = 1s, 2s$ ) is the one-electron variational wave function of the triplet or singlet metastable state of helium obtained by Winter and Lin [21]. The function  $\mathcal{F}_{\mathbf{k}_\alpha}^{(+)}$  is written as

$$\mathcal{F}_{\mathbf{k}_\alpha}^{(+)}(\mathbf{R}) = \exp[i\mathbf{k}_\alpha \cdot \mathbf{R}]. \quad (3)$$

The final wave function is chosen as [4]

$${}^S\xi_\beta^{(-)} = {}^S\Phi_\beta(\mathbf{r}_1, \mathbf{r}_2, \boldsymbol{\rho}_1, \boldsymbol{\rho}_2) \mathcal{F}_{\mathbf{k}_\beta}^{(-)}(\mathbf{R}) \quad (4)$$

with

$$\begin{aligned} {}^S\Phi_\beta(\mathbf{r}_1, \mathbf{r}_2, \boldsymbol{\rho}_1, \boldsymbol{\rho}_2) = & \frac{1}{\sqrt{2}} \{ \Psi_\beta(\boldsymbol{\rho}_1) \mathcal{F}_{\mathbf{k}_\beta}^{(-)}(\mathbf{r}_1) \tilde{\varphi}_{N_f L_f M_f}(\mathbf{r}_2) \\ & + (-1)^S \Psi_\beta(\boldsymbol{\rho}_2) \mathcal{F}_{\mathbf{k}_\beta}^{(-)}(\mathbf{r}_2) \tilde{\varphi}_{N_f L_f M_f}(\mathbf{r}_1) \}. \end{aligned} \quad (5)$$

${}^S\xi_\beta^{(-)}$  describes the positronium atom and the residual target bound state in the final channel of the reaction and distortions are introduced through the Coulomb wave functions  $\mathcal{F}_{\mathbf{k}_\beta}^{(-)}$ .  $\Psi_\beta$  is the final bound wave function of the positro-

nium atom [only the ground state  $\text{Ps}(1s)$  is considered in the present paper] and  $\tilde{\varphi}_{N_f L_f M_f}$  is the wave function of  $\text{He}^+$  in the state with quantum numbers  $(N_f, L_f, M_f)$ . The  $\mathcal{F}_{\mathbf{k}_\beta}^{(-)}$  Coulomb wave functions are given by

$$\mathcal{F}_{\mathbf{k}_\beta}^{(-)}(\mathbf{R}) = N_{\beta_+} \exp\left[i \frac{\mathbf{k}_\beta \cdot \mathbf{R}}{\mu_\beta}\right] {}_1F_1\left(i\beta_+; 1; -i \frac{\mathbf{k}_\beta \cdot \mathbf{R}}{\mu_\beta} - i \frac{k_\beta R}{\mu_\beta}\right), \quad (6)$$

$$\mathcal{F}_{\mathbf{k}_\beta}^{(-)}(\mathbf{r}_j) = N_{\beta_-} \exp\left[i \frac{\mathbf{k}_\beta \cdot \mathbf{r}_j}{\mu_\beta}\right] {}_1F_1\left(-i\beta_-; 1; -i \frac{\mathbf{k}_\beta \cdot \mathbf{r}_j}{\mu_\beta} - i \frac{k_\beta r_j}{\mu_\beta}\right), \quad j=1,2, \quad (7)$$

$\mathbf{k}_\alpha$  and  $\mathbf{k}_\beta$  being the wave vectors for the reduced positron in the entry channel and for the reduced positronium atom in the final channel, respectively. Moreover, the following quantities have been defined [4],

$$\beta_+ \approx \beta_- = \frac{(Z+1)\mu_\beta}{k_\beta}, \quad (8)$$

where  $Z$  is the ionicity of the target. In this paper,  $Z=0$  (neutral target). This is why the function  $\mathcal{F}_{\mathbf{k}_\alpha}^{(+)}(\mathbf{R})$  in Eq. (1) reduces to a plane wave. The reduced masses are  $\mu_\alpha \approx 1$  and  $\mu_\beta \approx 2$  and the normalization factors  $N_{\beta_\pm}$  are given by

$$N_{\beta_\pm} = \Gamma(1 \mp i\beta_\pm) \exp\left(\mp \frac{\pi}{2} \beta_\pm\right). \quad (9)$$

Finally, the perturbation potential and the CDW-FS-4b matrix element are given by

$$V_\alpha = \frac{2}{R} - \frac{1}{\rho_1} - \frac{1}{\rho_2} \quad (10)$$

and

$${}^S T_{\alpha\beta}^{(-)} = \langle {}^S \xi_\beta^{(-)} | V_\alpha | {}^S \xi_\alpha^{(+)} \rangle. \quad (11)$$

In particular, the CBA approximation is obtained by setting  $\beta_+ = \beta_- = 0$ .

The CDW-FS-4b matrix element may be rewritten as

$${}^S T_{\alpha\beta}^{(-)} = {}^S t_{1s2s} + (-1)^S {}^S t_{2s1s}, \quad (12)$$

$${}^S t_{ij} = \int d\mathbf{R} \mathcal{F}_{\mathbf{k}_\beta}^{(-)*}(\mathbf{R}) {}^S V_T^{ij}(\mathbf{R}) \mathcal{F}_{\mathbf{k}_\alpha}^{(+)}(\mathbf{R}) \quad (13)$$

and

$$\begin{aligned}
 {}^S V_T^{ij}(\mathbf{R}) &= \int d\mathbf{r}_1 \Psi_\beta^*(\boldsymbol{\rho}_1) \mathcal{F}_{\mathbf{k}_\beta}^{(-)*}(\mathbf{r}_1) \left( \frac{1}{R} - \frac{1}{\rho_1} \right) {}^S \varphi_i(\mathbf{r}_1) \\
 &\times \int d\mathbf{r}_2 \tilde{\varphi}_{N_f L_f M_f}^*(\mathbf{r}_2) {}^S \varphi_j(\mathbf{r}_2) \\
 &+ \int d\mathbf{r}_1 \Psi_\beta^*(\boldsymbol{\rho}_1) \mathcal{F}_{\mathbf{k}_\beta}^{(-)*}(\mathbf{r}_1) {}^S \varphi_i(\mathbf{r}_1) \\
 &\times \int d\mathbf{r}_2 \tilde{\varphi}_{N_f L_f M_f}^*(\mathbf{r}_2) \left( \frac{1}{R} - \frac{1}{\rho_2} \right) {}^S \varphi_j(\mathbf{r}_2) \\
 &= \left\{ \int d\mathbf{r}_1 \Psi_\beta^*(\boldsymbol{\rho}_1) \mathcal{F}_{\mathbf{k}_\beta}^{(-)*}(\mathbf{r}_1) \left( \frac{1}{R} - \frac{1}{\rho_1} \right) {}^S \varphi_i(\mathbf{r}_1) \right\} \\
 &\times \langle N_f L_f M_f | S j \rangle \\
 &+ \left\{ \int d\mathbf{r}_1 \Psi_\beta^*(\boldsymbol{\rho}_1) \mathcal{F}_{\mathbf{k}_\beta}^{(-)*}(\mathbf{r}_1) {}^S \varphi_i(\mathbf{r}_1) \right\} \\
 &\times {}^S \mathcal{K}_{N_f L_f M_f}^j(\mathbf{R}) = {}^S V_{T-cap}^{ij}(\mathbf{R}) + {}^S V_{T-exc}^{ij}(\mathbf{R}).
 \end{aligned} \tag{14}$$

According to this, the matrix element  ${}^S t^{ij}$  may be expressed as

$${}^S t^{ij} = {}^S t_{cap}^{ij} + {}^S t_{exc}^{ij}. \tag{15}$$

The matrix elements  ${}^S t_{cap}^{ij}$  and  ${}^S t_{exc}^{ij}$  may be obtained replacing  ${}^S V_T^{ij}$  in Eq. (13) by  ${}^S V_{T-cap}^{ij}$  and  ${}^S V_{T-exc}^{ij}$ , respectively.

As it was explained in I, the present CDW-FS-4b approximation describes capture and simultaneous excitation of the target. Considering Eqs. (13) and (14), it can be seen that both processes are produced simultaneously at each  $\mathbf{R}$  position. In other words and within a time-dependent representation, capture and excitation are produced in a simultaneous way, time to time, during all the collision reaction.

As both electrons are indistinguishable, the matrix element  ${}^S T_{\alpha\beta}^{(-)}$  in Eq. (12) is the coherent sum of two terms.  ${}^S t^{2s1s}$  describes the capture by the incident positron of an electron initially in the  $2s$  state of the helium atom to form  $\text{Ps}(1s)$  with simultaneous excitation of the electron initially in the  $1s$  state of the target to a final state  $\text{He}^+(N_f L_f M_f)$ . For future reference, this process is labeled by  $f$ . In an analogous way,  ${}^S t^{1s2s}$  describes the capture of a  $1s$  electron to form  $\text{Ps}(1s)$  with simultaneous excitation of a  $2s$  electron to the same final state  $(N_f L_f M_f)$  of  $\text{He}^+$  and the process is labeled by  $g$ . Both processes  $f$  and  $g$  lead to same final state and therefore are summed coherently. These processes are sketched in Fig. 2.

In order to evaluate the CDW-FS-4b matrix element, a partial-wave expansion technique has been used. By using  ${}^S \varphi_i(\mathbf{r}) = {}^S R_i(r) Y_{00}(\hat{\mathbf{r}})$  with  $i=1s$  or  $2s$ ,  $\tilde{\varphi}_{N_f L_f M_f}(\mathbf{r}) = \tilde{R}_{N_f L_f}(r) Y_{L_f M_f}(\hat{\mathbf{r}})$ , and  $\Psi_\beta(\boldsymbol{\rho}) = \tilde{R}_{1s}(\rho) Y_{00}(\hat{\boldsymbol{\rho}})$  and the following development,

$$\mathcal{F}_{\mathbf{k}}^{(\pm)}(\mathbf{r}) = \sum_{lm} 4\pi(i)^l e^{\pm i\delta_l} \frac{1}{kr} F_l(kr) Y_{lm}^*(\hat{\mathbf{k}}) Y_{lm}(\hat{\mathbf{r}}) \tag{16}$$

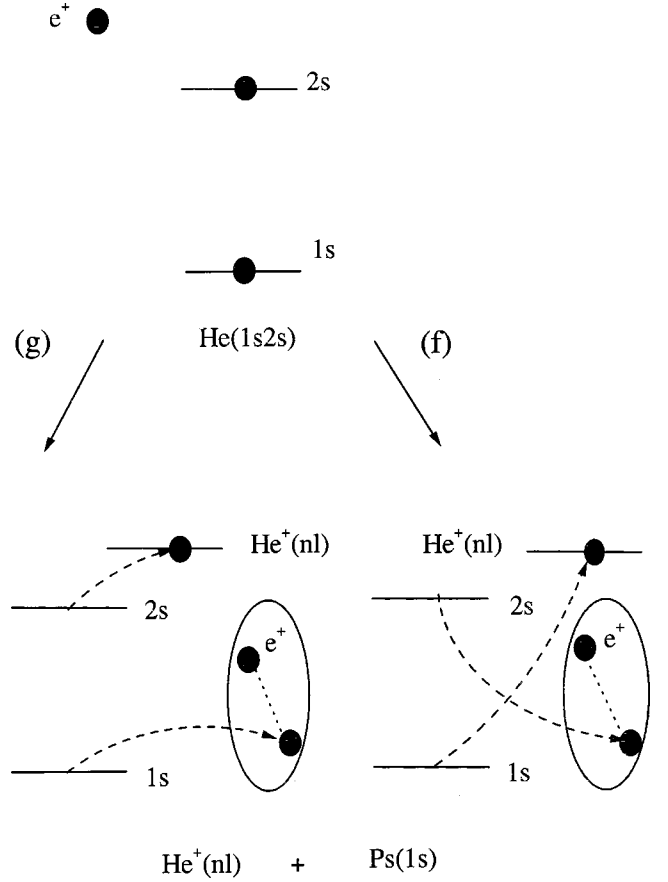


FIG. 2. Processes  $f$  and  $g$ .

the quantity  ${}^S \mathcal{K}_{N_f L_f M_f}^i$  appearing in Eq. (14) may be rewritten as

$${}^S \mathcal{K}_{N_f L_f M_f}^i(\mathbf{R}) = {}^S \mathcal{L}_{N_f L_f}^i(R) Y_{L_f M_f}^*(\hat{\mathbf{R}}) \tag{17}$$

with

$$\begin{aligned}
 {}^S \mathcal{L}_{N_f L_f}^i(R) &= \sqrt{4\pi} \hat{L}_f \int_0^\infty dr r^2 \tilde{R}_{N_f L_f}(r) \\
 &\times \left( \frac{r_{<}^{L_f}}{r_{>}^{L_f+1}} - \frac{\delta_{L_f 0}}{R} \right) {}^S R_i(r),
 \end{aligned} \tag{18}$$

where we use the convention  $\hat{l} = 2l + 1$ ,  $r_{<} = \min(r, R)$ , and  $r_{>} = \max(r, R)$ .

Differential and total cross sections for an excited electron of quantum numbers  $N_f L_f M_f$  are given by

$$\left[ \frac{d\sigma}{d\Omega} \right]_{N_f L_f M_f}^S = \frac{1}{4\pi^2} \frac{k_\beta}{k_\alpha} \mu_\alpha \mu_\beta |{}^S T_{\alpha\beta}^{(-)}|^2 \tag{19}$$

and

$${}^S \sigma_{N_f L_f M_f} = \int d\Omega \left[ \frac{d\sigma}{d\Omega} \right]_{N_f L_f M_f}^S. \tag{20}$$

We have also

$${}^S\sigma_{N_f L_f} = \sum_{M_f} {}^S\sigma_{N_f L_f M_f}. \quad (21)$$

Finally, the polarization fraction of the  $2p-1s$  multiplet line of  $\text{He}^+$  is given by

$${}^S P = \frac{{}^S\sigma_{2p_0} - {}^S\sigma_{2p_1}}{{}^S\sigma_{2p_0} + {}^S\sigma_{2p_1}}. \quad (22)$$

Two cases have to be considered.

### A. $L_f \neq 0$

In this case, the scalar product  $\langle N_f L_f M_f | S j \rangle$  with  $j=1s$  or  $2s$  is zero and only the second part of the expression (14) must be evaluated, i.e.,  ${}^S t_{exc}^{ij}$ . We have

$${}^S T_{\alpha\beta}^{(-)} = {}^S t_{exc}^{ij} + (-1)^S {}^S t_{exc}^{ji}, \quad (23)$$

$${}^S T_{\alpha\beta}^{(-)} = \frac{1}{2} \mathcal{B} \sum_{l_i} i^{l_i} e^{i\delta_{l_i}} \hat{l}_i \hat{L}^{1/2} [{}^S \tilde{\mathcal{U}}_{l_i L}^{1s2s} + (-1)^S {}^S \tilde{\mathcal{U}}_{l_i L}^{2s1s}] Y_{L-M_f}(\hat{\mathbf{k}}_\beta) \quad (24)$$

with

$$\mathcal{B} = \frac{(4\pi)^{3/2}}{k_\alpha k_+ k_-} \quad (25)$$

and

$${}^S \tilde{\mathcal{U}}_{l_i L}^{ij} = \sum_{l_f} i^{-l-l_f} e^{i(\delta_{l_i} + \delta_{l_f})} (-1)^{l+l_f} \tilde{\mathcal{A}}_{l_i L}^{l l_f L} {}^S \tilde{\mathcal{R}}_{l_i l_f}^{ij} \quad (26)$$

with

$$\begin{aligned} \tilde{\mathcal{A}}_{l_i L}^{l l_f L} &= \hat{l}_f \begin{pmatrix} l & l_f & L \\ 0 & 0 & 0 \end{pmatrix} \begin{pmatrix} l_i & L_f & L \\ 0 & -M_f & M_f \end{pmatrix} \\ &\times \left[ \sum_{\tilde{L}} (-1)^{\tilde{L}} \tilde{\mathcal{L}} \begin{pmatrix} l & L_f & \tilde{L} \\ 0 & 0 & 0 \end{pmatrix} \begin{pmatrix} l_f & \tilde{L} & l_i \\ 0 & 0 & 0 \end{pmatrix} \right. \\ &\left. \times \begin{pmatrix} l_i & L_f & L \\ l & l_f & \tilde{L} \end{pmatrix} \right], \quad (27) \end{aligned}$$

$${}^S \tilde{\mathcal{R}}_{l_i l_f}^{ij} = \int_0^\infty dR F_{l_f}(k_+ R) {}^S \tilde{\mathcal{V}}_l^{ij}(R) F_{l_i}(k_\alpha R), \quad (28)$$

$${}^S \tilde{\mathcal{V}}_l^{ij}(R) = \left\{ \int_0^\infty dr r F_l(k_- r) \tilde{\mathcal{J}}_l(r; R) {}^S R_l(r) \right\} \mathcal{L}_{N_f L_f}^j(R), \quad (29)$$

$$\tilde{\mathcal{J}}_l(r; R) = \frac{1}{2} \int_{-1}^{+1} du \tilde{\mathcal{R}}_{1s}(\rho) P_l(u), \quad (30)$$

and

$$\rho = (r^2 + R^2 - 2rRu)^{1/2}. \quad (31)$$

The functions  $F_l(k_\pm r)$  and  $F_l(k_\alpha r)$  are the Coulomb radial functions with the Sommerfeld parameters  $\eta = \beta_\pm$  and  $\eta = \nu_\alpha = 0$  (in this case, the Coulomb function reduces to a plane wave), respectively [see Eq. (8)]. The phase shifts,  $\delta_l$  are the usual Coulomb phase shifts  $\delta_l = \arg \Gamma(l+1+i\eta)$  and  $P_l$  indicates the Legendre polynomial of degree  $l$ .

### B. $L_f = 0$

In this case, the scalar product  $\langle N_f L_f M_f | S j \rangle$  with  $j=1s$  or  $2s$  is not zero and the two parts of the expression (14) must be evaluated. However, due to the selection rules of the Clebsh-Gordon coefficients, the difficulty is reduced since  $L=l_i$ . We have

$${}^S t_{cap}^{ij} = \mathcal{B} \sum_{l_i} i^{l_i} e^{i\delta_{l_i}} \hat{l}_i^{1/2} {}^S \mathcal{U}_{l_i}^{ij} Y_{l_i 0}(\hat{\mathbf{k}}_\beta) \quad (32)$$

with

$${}^S \mathcal{U}_{l_i}^{ij} = \sum_{l_f} i^{-l-l_f} e^{i(\delta_{l_i} + \delta_{l_f})} \mathcal{A}_{l_i}^{l l_f} {}^S \mathcal{R}_{l_i l_f}^{ij} \quad (33)$$

with

$$\mathcal{A}_{l_i}^{l l_f} = \hat{l}_f \begin{pmatrix} l_i & l & l_f \\ 0 & 0 & 0 \end{pmatrix}^2, \quad (34)$$

$${}^S \mathcal{R}_{l_i l_f}^{ij} = \int_0^\infty dR F_{l_f}(k_+ R) {}^S \mathcal{V}_l^{ij}(R) F_{l_i}(k_\alpha R), \quad (35)$$

and

$${}^S \mathcal{V}_l^{ij}(R) = \left\{ \int_0^\infty dr r F_l(k_- r) \mathcal{J}_l(r; R) {}^S R_l(r) \right\} {}^S \mathcal{W}_{N_f}^j, \quad (36)$$

with

$$\mathcal{J}_l(r; R) = \frac{1}{2} \int_{-1}^{+1} du \tilde{\mathcal{R}}_{1s}(\rho) \left( \frac{1}{R} - \frac{1}{\rho} \right) P_l(u) \quad (37)$$

and

$${}^S \mathcal{W}_{N_f}^j = \langle N_f L_f M_f | S j \rangle. \quad (38)$$

Similarly, the expression  ${}^S t_{exc}^{ij}$  reduces to

$${}^S t_{exc}^{ij} = \mathcal{B} \sum_{l_i} i^{l_i} e^{i\delta_{l_i}} \hat{l}_i^{1/2} {}^S \tilde{\mathcal{U}}_{l_i}^{ij} Y_{l_i 0}(\hat{\mathbf{k}}_\beta) \quad (39)$$

with

$${}^S \tilde{\mathcal{U}}_{l_i}^{ij} = \sum_{l_f} i^{-l-l_f} e^{i(\delta_{l_i} + \delta_{l_f})} \mathcal{A}_{l_i}^{l l_f} {}^S \tilde{\mathcal{R}}_{l_i l_f}^{ij} \quad (40)$$

leading to

$$S_{ij} = S_{i_{cap}}^{ij} + S_{i_{exc}}^{ij} = \mathcal{B} \sum_{l_i} i^{l_i} e^{i\delta_{l_i}} \hat{l}_i^{1/2} {}^S \mathcal{T}_{l_i}^{ij} Y_{l_i 0}(\hat{\mathbf{k}}_\beta) \quad (41)$$

and

$$S_{\alpha\beta}^{(-)} = \frac{1}{2} \mathcal{B} \sum_{l_i} i^{l_i} e^{i\delta_{l_i}} \hat{l}_i^{1/2} [{}^S \mathcal{T}_{l_i}^{1s2s} + (-1)^S {}^S \mathcal{T}_{l_i}^{2s1s}] Y_{l_i 0}(\hat{\mathbf{k}}_\beta) \quad (42)$$

with

$${}^S \mathcal{T}_{l_i}^{ij} = S \mathcal{U}_{l_i}^{ij} + S \tilde{\mathcal{U}}_{l_i}^{ij}. \quad (43)$$

In particular

$$\begin{aligned} {}^S \sigma_{2s} = & \mathcal{C} \sum_{l_i} \hat{l}_i |{}^S \mathcal{T}_{l_i}^{1s2s}|^2 + \mathcal{C} \sum_{l_i} \hat{l}_i |{}^S \mathcal{T}_{l_i}^{2s1s}|^2 \\ & + 2\mathcal{C}(-1)^S \sum_{l_i} \{ \text{Re}[{}^S \mathcal{T}_{l_i}^{1s2s}] \text{Re}[{}^S \mathcal{T}_{l_i}^{2s1s}] \\ & + \text{Im}[{}^S \mathcal{T}_{l_i}^{1s2s}] \text{Im}[{}^S \mathcal{T}_{l_i}^{2s1s}] \} \end{aligned} \quad (44)$$

with

$$\mathcal{C} = \frac{4\pi k_\beta \mu_\alpha \mu_\beta}{k_\alpha^3 k_+^2 k_-^2}. \quad (45)$$

Note that  ${}^S \sigma_{2s}$  has the form  $|f + (-1)^S g|^2$  revealing interference effects between the processes  $f$  and  $g$ . Unfortunately, it was not possible to reduce  ${}^S \sigma_{2p_m}$  to a similar simple expression.

### III. RESULTS

In Figs. 3(a), 3(b), 3(c), and 3(d), CDW-FS-4b and CBA total Ps( $1s$ ) cross sections (TCS) with metastable helium targets as a function of the impact energy are presented for the  $1s$ ,  $2s$ ,  $2p_0$ , and  $2p_1$  final states of the residual target  $\text{He}^+$ , respectively.

It can be seen from the figures that there is no threshold for the transfer-excitation process studied if the final residual target is left in a  $1s$  state. On the contrary, for final  $n=2$  states, there is a threshold at about 40 eV. The threshold may be obtained by using the energy-conservation law resulting in 38 and 39 eV for the initial singlet and triplet term of the target, respectively.

In general, for a given target initial term (singlet or triplet) and a given final residual target state, the CDW-FS-4b cross sections are lower than the CBA ones as the impact energy increases. It may be also seen from the figures that except for the  $\text{He}^+(1s)$  final residual target state, cross sections corresponding to triplet states dominate over the ones corresponding to singlet states at high impact energy.

In Figs. 4(a) and 4(b), the contribution of the processes  $f$  and  $g$  aboved defined to the CDW-FS-4b TCS is analyzed for the  $2s$  and  $2p_0$  final states of the residual target, respectively, for the case of the triplet initial term. For the  $2s$  final state, the process  $f$  is negligible being the process  $g$  almost

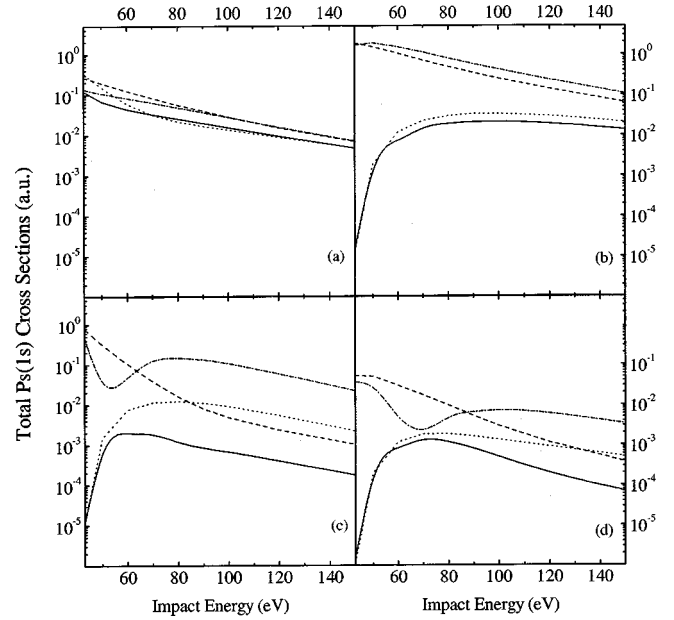


FIG. 3. Total Ps ( $1s$ ) cross sections for several  $\text{He}^+$  final residual target states. (a)  $\text{He}^+(1s)$ . Initial singlet state: CDW-FS-4b, full line; CBA, dashed line. Initial triplet state: CDW-FS-4b, dotted line; CBA, dashed and dotted line. (b) Same as (a) but for  $\text{He}^+(2s)$  final residual target state. (c) Same as (a) but for  $\text{He}^+(2p_0)$  final residual target state. (d) Same as (a) but for  $\text{He}^+(2p_1)$  final residual target state.

responsible for the TCS. This may be explained in the following way. In the process  $f$ , the  $2s$  target electron is captured and the  $1s$  target electron has to be promoted to a  $2s$  state of  $\text{He}^+$ . On the contrary, in the process  $g$  the  $1s$  target electron is captured and the remaining  $2s$  target electron relaxes to a  $2s$  state of  $\text{He}^+$ , which is more convenient taking into account the overlap between initial and final wave functions. Although not shown here, the same is true for initial singlet terms and for CBA TCS. For final state  $\text{He}^+(1s)$ , the situation is the opposite: the process  $f$  dominates over the process  $g$ . In considering the  $2p_0$  final state, both  $f$  and  $g$  processes may be, depending on the incident energy, of the same magnitude, and the total cross section resulting from their coherent sum evidences an interference effect. The same is true for the  $2p_1$  final state.

Let us consider now the cross sections as the impact energy increases. It can be seen from the Fig. 3 that the limit value of the CDW-FS-4b or CBA cross sections at the higher energies considered is different for the singlet or triplet initial term. However, the difference is quite small for the  $1s$  final state of the residual target and bigger for the  $2s$  and  $2p$  final excited states of  $\text{He}^+$  being much more pronounced in the latter ones. For  $2p$  final states, the gap between the TCS corresponding to singlet and triplet initial terms, resembles, in some way, the behavior of the TCS for excitation of helium atoms by electron impact. For instance, the excitations corresponding to the transitions  $2^1S \rightarrow 3^1P$  and  $2^3S \rightarrow 3^3P$  [22] have different TCS as the impact energy increases although the singlet term dominates the TCS whereas in this paper the inverse is true.

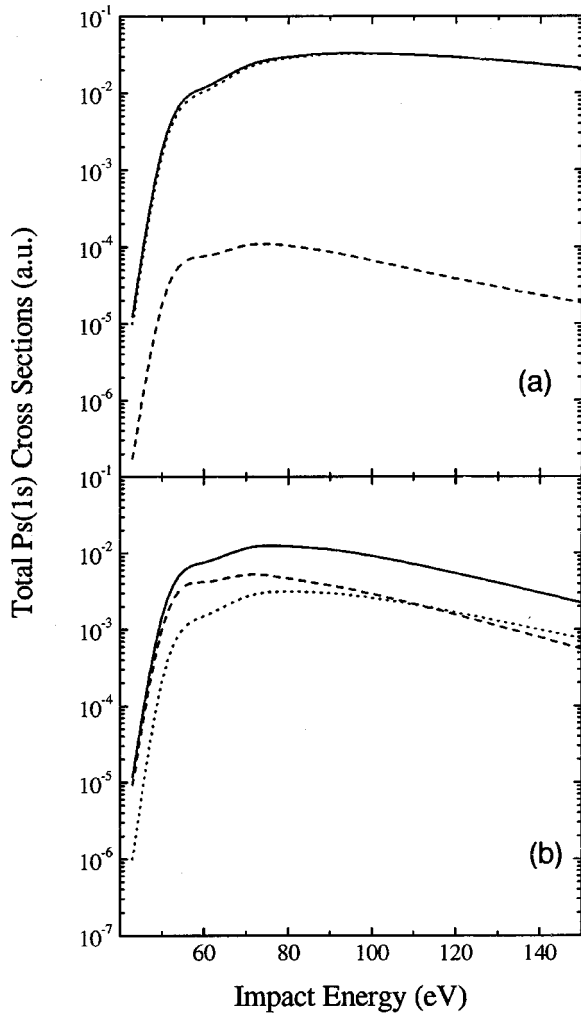


FIG. 4.  $f$  and  $g$  processes in the CDW-FS-4b approximation. Results for initial triplet term and for (a)  $\text{He}^+(2s)$  and (b)  $\text{He}^+(2p_0)$  final states. CDW-FS-4b, full line. TCS corresponding to  $f$  process, dashed line. TCS corresponding to  $g$  process, dotted line.

As the energy impact increases, the transfer process leaving the residual target in a  $2s$  state becomes dominant independently of the initial target term. As explained above, for the final  $2s$  ( $1s$ ) state the process  $g$  ( $f$ ) dominates the reaction. In particular, TCS for the final  $\text{He}^+(1s)$  state are lower than the ones corresponding to  $\text{He}^+(2s)$ . This may be understood by using matching velocity arguments for the capture process and taking into account the overlap of initial and final wave functions given by the term  $\langle N_f L_f M_f | S_j \rangle$  [both terms of Eq. (14) collaborate in this case as  $L_f \neq 0$ ]. As it is well known [7], electron capture at intermediate and high impact energies is more probable to occur when the projectile velocity is close to the mean orbital velocity of the electron to be captured. Then, capture from an  $1s$  orbital is more favorable at energies higher than the ones corresponding to capture from a  $2s$  orbital. Therefore, as the impact energy increases, capture from the  $1s$  orbital of the initial ( $1s2s$ ) electronic configuration of the helium atom becomes dominant. The remaining electron is left in an excited  $2s$  state of the  $\text{He}^+$  residual target that overlaps the  $2s$  orbital of the

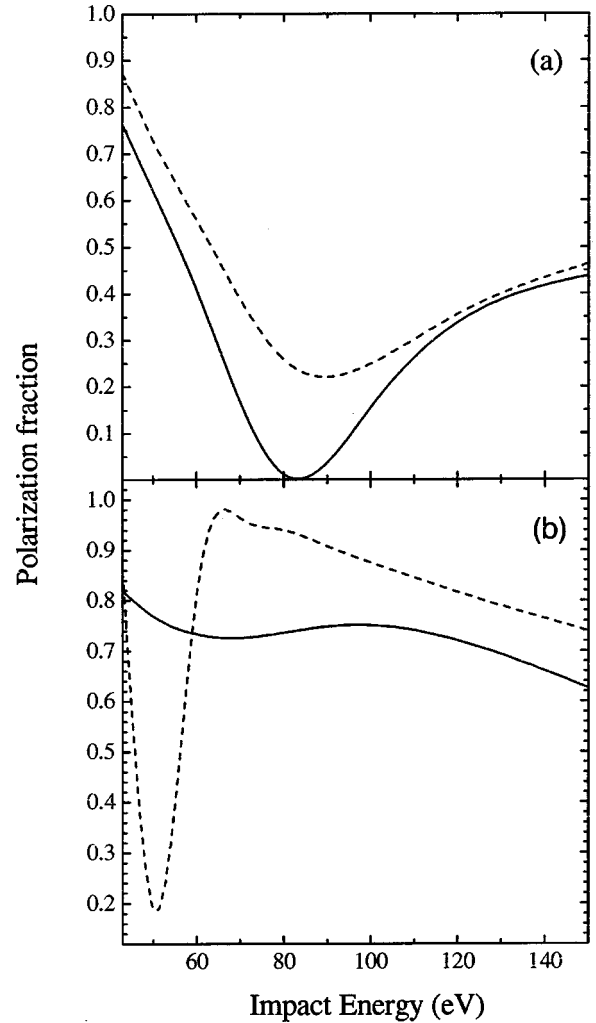


FIG. 5. Polarization fraction. (a) Initial singlet state. (b) Initial triplet state. CDW-FS-4b, full line. CBA, dashed line.

helium atom in a better way than the  $1s$  state of  $\text{He}^+$ .

This behavior of the cross section is different from the one observed for positronium formation with an ( $1s^2$ ) electronic initial configuration of the helium atom leaving the residual target in a  $2s$  state. This process has been studied in I and it has been shown that it is almost negligible as the impact energy increases. The reason is that in that case one of the electrons is captured essentially by re-arrangement (the overlap between  $2s$  final and  $1s$  initial states is rather small) while the other must be excited to an  $2s$  state through an optically forbidden transition. In the present case, the non-captured electron is in a  $2s$  state of the helium atom (as discussed above, process  $g$  is dominant in this case) and suffers a transition to a  $2s$  state of the  $\text{He}^+$ .

In relation to  $2p$  final residual target states, the polarization fraction of the  $2p-1s$  multiplet line of  $\text{He}^+$  defined in Eq. (22) may be useful in experiments to be made. By measuring the polarization of the light emitted through the decaying of the residual target to its ground state, information about the population of the  $2p$  final states produced during the collision may be obtained. In Figs. 5(a) and 5(b), the CDW-FS-4b and CBA predictions for the polarization frac-



tion of the  $2p-1s$  multiplet line of  $\text{He}^+$  are shown for the initial singlet and triplet terms, respectively. In the case of a singlet, CDW-FS-4b and CBA results are similar in shape. On the contrary, they are quite different for the triplet term. In both cases, the polarization fraction is always positive.

#### IV. CONCLUSIONS AND PERSPECTIVES

The CDW-FS-4b model has been applied to study positronium formation in ground state through charge transfer and simultaneous excitation of helium targets initially in the  $2^1S$  (singlet) and  $2^3S$  (triplet) metastable states by impact of fast positrons. For  $\text{He}^+(2p)$  final residual target states, interesting interference effects in the TCS have been found. It has been shown that at high impact energies, the channel leading to  $\text{He}^+(2s)$ , as a final residual target, becomes preferential. The same reaction was studied in I for helium atoms in a ground state. In this case, the preferred residual target was  $\text{He}^+(1s)$ . At the higher impact energies studied, TCS for the analyzed metastable states of the target are at most 5–10% of the ones corresponding to helium atoms in a ground state. As discussed in I, the contribution of the transfer-excitation pro-

cess to the  $\text{Ps}(1s)$  formation is more important for other  $ns^2$  targets such as the alkaline-earth metals. The contribution to the  $\text{Ps}(1s)$  formation coming from excited states of these targets may also play a more prominent role than they do in helium. This could be also the case for other two-active electron systems such as multicharged ions for which metastable species are present in a high proportion in the obtained beams [19]. This is matter of future work.

#### ACKNOWLEDGMENTS

Fruitful discussions with César Ramírez are acknowledged. This work was partially supported by the French-Argentinean ECOS-Sud program (No. A98E06). O.A.F. and R.D.R. also acknowledge support from the Agencia Nacional de Promoción Científica y Tecnológica (BID 802/OC-AR PICT No. 03-04262) and the Consejo Nacional de Investigaciones Científicas y Técnicas de la República Argentina. The authors would like to thank the CINES (Center Informatique National de l'Enseignement Supérieur) for providing free computer time.

- 
- [1] B. H. Bransden and J. C. Noble, *Adv. At., Mol., Opt. Phys.* **32**, 19 (1994).
- [2] G. Laricchia, in *Proceedings of the 19th International Conference on Physics of Electronic and Atomic Collisions, Whistler*, edited by L. J. Dubé, J. Brian, A. Mitchell, J. William McConkey, and C. E. Brion (AIP, Woodbury, NY, 1995), p. 385, book of contributed papers.
- [3] O. A. Fojón, Ph.D. thesis, Universidad Nacional de Rosario, 1994 (unpublished).
- [4] O. A. Fojón, R. D. Rivarola, R. Gayet, J. Hanssen, and P. A. Hervieux, *Phys. Rev. A* **54**, 4923 (1996).
- [5] O. A. Fojón, R. D. Rivarola, R. Gayet, J. Hanssen, and P. A. Hervieux, *J. Phys. B* **30**, 2199 (1997).
- [6] C. R. Mandal, S. C. Mandal Mita ans Mukherjee, *Phys. Rev. A* **44**, 2968 (1991).
- [7] J. Hanssen, P. A. Hervieux, O. A. Fojón, R. D. Rivarola, and R. Gayet, *J. Phys. B* **31**, 1313 (1998).
- [8] O. A. Fojón, R. Gayet, J. Hanssen, and R. D. Rivarola, *Phys. Scr.* **51**, 204 (1995); **52**, 607 (1995).
- [9] L. Diana, P. Coleman, D. Brooks, P. Pendleton, and D. Norman, *Phys. Rev. A* **34**, 2731 (1986).
- [10] M. Overton, R. J. Mills, and P. G. Coleman, *J. Phys. B* **26**, 3951 (1993).
- [11] D. R. Schultz and R. E. Olson *Phys. Rev. A* **38**, 1866 (1988); D. R. Schultz, C. O. Reinhold, and R. E. Olson, *ibid.* **40**, 4947 (1989).
- [12] B. H. Bransden, C. J. Joachain, and J. F. McCann, *J. Phys. B* **25**, 4965 (1992).
- [13] P. Mandal, A. S. Ghosh, and N. C. Sil, *J. Phys. B* **8**, 2377 (1975).
- [14] R. N. Hewitt, C. J. Noble, and B. H. Bransden, *J. Phys. B* **25**, 557 (1992).
- [15] S. K. Adhikari and A. S. Ghosh, *Chem. Phys. Lett.* **262**, 460 (1996).
- [16] P. Chaudhuri, S. K. Adhikari, and A. S. Ghosh, *J. Phys. B* **30**, L81 (1997).
- [17] P. Chaudhuri and S. K. Adhikari, *Phys. Rev. A* **57**, 984 (1998).
- [18] O. A. Fojón, R. D. Rivarola, J. Hanssen, and P. A. Hervieux, *J. Phys. B* (to be published).
- [19] S. Bliman, M. G. Suraud, D. Ditz, and B. A. Huber, *Phys. Rev. A* **46**, 1321 (1992).
- [20] R. S. Van Dyck Jr., C. E. Johnson, and H. A. Shugart, *Phys. Rev. A* **4**, 1327 (1971).
- [21] T. G. Winter and C. C. Lin, *Phys. Rev. A* **12**, 434 (1975).
- [22] N. F. Mott and H. S. W. Massey, *The Theory of Atomic Collisions* (Oxford University Press, Oxford, 1965).